Mitigating climate change damage on heritage structures by continuous conservation management using thermal monitoring

Abstract

Climate change and anthropogenic causes represent a multidisciplinary problem in urban environments, specifically in the destruction of historical elements of enormous value. Although conventional methods are based on comprehensive conservation measures and periodic inspection, these urban elements sometimes lie in a state of neglect due to lack of means to carry out continuous monitoring. The present work develops a replicable and easy-to-apply multi-analytical methodology, which proposes the use of standard monitoring to automatically diagnose the elements of heritage buildings. It is based on the development of an inverse characterization model of the thermal response in a known state of conservation through standard monitoring. The use of standard monitoring as a development variable will facilitate its obtaining. The methodology involves characterising energy response to environmental excitations measured against what is deemed to be a baseline state of conservation. Anomalies detected in the comparison of the baseline to subsequent real-time measurements would alert the need to bring scheduled on-site inspections forward with an affordable cost. The methodology developed was validated on a real urban element. The findings revealed a good fit between calculated and experimental data, with mean absolute errors of under 1°C in both seasons. The proposal can be applied in other fields such as preventive maintenance.

Keywords: heritage buildings; impact of climate; preventive conservation; inverse model; historic preservation

;

Nomenclature

Variable/Acronym/ Abbreviation	Description	Units
UNESCO	United Nations Educational, Scientific and Cultural Education	-
J	International System – energy units - Joule	-
kg	International System< – mass units - kilograms	-
m^2	International System – surface units – square meters	-
K	International System – temperature units – Kelvin	-
W	International System – power units – Watt	-
m	International System – length units – meter	-
Q_{SE-i}	Heat flux due to solar irradiation on Surface i	W/m^2
Q_{CV-i}	Heat flux due to air convection on Surface i	W/m^2
Q_{RD-i}	Heat flux due to longwave radiation exchange in Surface i	W/m^2
Q_{CD}	Heat conduction in the interior of the wall	W/m^2
T_i	The representative temperature of the Surface i	ºC
α_i	The absorptivity of the surface i	-
I_{RR-i}	The incident global radiation on the surface i	W/m^2
h_{CV-i}	Heat convection coefficient on Surface i	$W/K{\cdot}m^2$
T_{AIR}	The representative temperature of the air	ºC
h_{RD-i}	Radiation coefficient	$W/K{\cdot}m^2$
T_{RD}	The mean radiant temperature	ºC

T_{SKY}	The sky temperature	ºC
σ	The Stefan-Boltzmann constant adopts a value of $5.67 \cdot 10^{-7}$	$W/m^2 \cdot K^4$
ε_i	The surface's longwave emittance	-
k	The mean thermal conductivity	W/m·K
L	The wall thickness of the element	m
a_i, b_i, d_i, aa_i, bb_i, dd_i,	The coefficients of the baseline model	-
$Texc_i$	The temperature of external excitations on the surface i	ºC
ε_{SKY}	Sky emissivity	-
T_{DEW}	The dew-point temperature of outdoor air	K
$F_{Cloudiness}$	The cloudiness factor	-
E_N	Constant cloudiness parameter: 3 in summer and 5 in winter.	-
Err_{Ti}	Uncertainty of surface temperature calculated i	ºC
$\sigma(X)$	The standard deviations of variable X	
$T_{i-estimated}$	Final estimation of the baseline model for the temperature of surface i	ºC

1 Introduction

The contemporary approach to protecting, conserving and safeguarding the enormous historical and social value enshrined in the cultural heritage calls for furthering its use as a social heritage element and element for sustainable development (ICOMOS, 2005). Since this legacy is exposed to natural and anthropic risks (Silva et al., 2020a) that may compromise its integrity or accelerate its deterioration (Camuffo, n.d.), the definition of preventive conservation and maintenance strategies is of paramount importance (Icomos, 2000; Report, 2001). In light of the many heritage elements concerned and the paucity of government and/or private funding to ensure their conservation, more sustainable preservation based on prevention and continuous monitoring should be introduced (Canada, n.d.). Authors like Oliveira et al. test in their research the acute problem faced by the heritage elements. On the one hand, they studied the problem of atmospheric contaminations joined with bad conservation (Oliveira et al., 2020). In another hand, the acceleration of degradation due to the effects of nanoparticle deposition (Oliveira et al., 2019a, 2019b). The results of these authors (Silva et al., 2020a, 2020d) are even more alarming since they quantify the health risk posed by these particles for the people who visit these elements.

Further to a review by Ivan et al. (Fung et al., 2017), the number of scientific papers on historic building conservation has mushroomed of late. Zahirah et al. (Azizi et al., 2016) classified these papers by type of measures addressed: adaptation of historical buildings to a new use; or mere comprehensive rehabilitation. A third but no less important category, however, is the problem posed by the conservation of severely exposed historic heritage (Douglas-Jones et al., 2016) such as defensive walls and/or archaeological sites. Victoria et al. (Jenkins, 2018) showed that interest in the subject has been heightened with the advent of scientific and technical developments in building conservation. Marco et al. (Filippi, 2015), in turn, proposed a series of indicators to encourage renovation of pre-1945 buildings. According to their findings, rehabilitation can be broached as readily in historic as in conventional buildings, although heritage values must be borne in mind in the former.

So, Chiara et al. (Bertolin and Loli, 2018) concluded that the envelopes of these heritage elements must be addressed separately. Heritage element envelopes afford protection against environmental and anthropogenic excitations in buildings with a given use and constitute a key element in all types of intervention. On the one hand, the aesthetic values of envelopes must be preserved, particularly in singular buildings such as museums (Lucchi, 2018), fortress (Morillas et al., 2018; Silva et al., 2020b, 2020c), churches or historic cities (Morillas et al., 2019). Morillas et al. (Morillas et al., 2019, 2018) employ detailed techniques to characterize the interior of the solid media and diagnose the causes of degradation of different structures. Thanks to the methods they propose, it is possible to design the optimal solution for the rehabilitation of these elements. For its part, Silva et al. (Silva et al., 2020c, 2020b) studied in detail the effect of air pollution on fortress-type elements. On the other hand, Vasiliki et al. (Pachta and Papayianni, 2017) conducted an in-depth study of the materials that can be used in ecclesiastic buildings to minimise the impact on the initial construction. Their paper described the difficulties involved and the benefits of improving these structures with a view to their long-term conservation. Therefore, as Hugo et al. (Santos et al., 2017) stressed, building aesthetics are not only a parameter deemed by United Nations Educational, Scientific and Cultural Education (UNESCO) to be non-modifiable but define such heritage elements' cultural essence. Hulya et al. (Yüceer and Ipekoğlu, 2012) discussed the importance of the outer envelopes of historic heritage elements and proposed a methodology for upgrades deploying today's techniques and materials. On the other, neither the initial construction techniques nor the original materials should be overlooked. The primary problem lies in the outer surfaces. Xin-Yi et al. (Qian et al., 2015) analysed the issues encountered when cleaning and conserving the outermost layer of the envelope and the need to ensure its

protection against pollutant toxicity. Their paper identified the pursuit of natural surface treatments as a line of research on the rise. Such treatments are applied to surfaces at scheduled intervals or on an ad hoc basis where necessary and call for a continuous inspection by qualified technicians. Carmen et al. (Salazar-Hernández et al., 2015) proposed a chemical surface treatment that can be adapted to surface typologies and described experiments that attested to its good performance. Nonetheless, as in the preceding case, the technique requires continuous heritage element monitoring to define the timing of the next intervention.

The requirements before appear to suggest the need for preventive conservation focused on the outer surface of heritage elements, i.e., on the surface in contact with environmental and anthropogenic excitations. Preventive conservation applied to cultural heritage elements is understood to mean systematic and continuous action (Moioli et al., 2018). The respective model should identify, assess, detect and monitor heritage elements to eliminate or minimise the risk of deterioration, tackling the underlying cause to prevent degeneration, loss or costly rehabilitation (Fregonese et al., 2018). Herráez et al. (Plan and Preventive, 2011) defined the stages of preventive conservation: multidisciplinary analysis to assess heritage characteristics, state of conservation, use and management; analysis and proposal of urgent measures to minimise or mitigate risks; definition of risk incidence control and follow-up mechanisms before proposing systematic maintenance measures; and a protocol for continuous review. The literature on cultural heritage conservation from that perspective is expanding, with most articles based on case studies defining methodologies, standards, monitoring tools, measurement strategies and software (Bonora et al., 2019). Research on monitoring has been geared to controlling geomorphological risk and its effects on structural behaviour (Gentile and Saisi, 2013; Romero et al., 2018), with a growing number of papers on temperature and relative humidity. Gina et al. (Crevello et al., 2015) developed a method focusing on the need for continuous monitoring as an automatic diagnostic mechanism for detecting further damage to heritage elements.

According to the foregoing, any conservation procedure is incomplete in the absence of continuous heritage element monitoring and a procedure for analysing the experimental data by measuring the state of the historic heritage element's surface, before or after an intervention. Such monitoring of the surrounding microclimate and heritage elements' thermal response entails advantages when designing a protocol for automatic control and follow-up of heritage element conservation. Authors applying non-invasive techniques stress the advantages of preventive control and planning geared to mitigating risk factors (Fregonese et al., 2018; Mesas-Carrascosa et al., 2016; Varas-muriel and Fort, 2018). For that, a current that appears in the literature is that based primarily on the surface and air temperature and relative humidity is the approach most frequently described in the literature reviewed. It is due to be simple, non-invasive monitoring and with an affordable cost. Kordatos et al. (Kordatos et al., 2013) and Young et al. (Jo and Lee, 2014) performed continuous thermographic real-time monitoring to analyse conservation in murals, concluding that surface temperature is a sufficiently reliable parameter for diagnosing the condition of heritage elements. . So, many technological solutions are in place for the wireless monitoring of historic heritage elements and have been discussed by Josiah et al. (Hester et al., 2017). Such solutions are not non-invasive, however, nor do they establish mechanisms for data processing or data-based diagnosis. This type of methodologies requires many measurements. However, authors like Prieto et al. (Prieto et al., 2017) demonstrate that the results are satisfactory.

The literature review reveals the lack of inspection of these heritage elements by public institutions and the importance of reinforcing it. Oliveira et al. (Oliveira et al., 2020, 2019a) it quantifies the rapid degradation that priceless items are undergoing in Rome (Italy) or Granada (Italy); and the need to implement maintenance techniques. This is due to the lack of resources and the lack of knowledge of the personnel in charge of this responsibility. Also, the review shows

the use of thermal evaluation techniques since the thermal parameters (density, specific heat, conductivity, emissivity, etc.) are linked to the state of the property, both on the surface and inside it. Therefore, intending to develop a replicable and easy-to-apply methodology, this work proposes the use of standard monitoring to automatically diagnose the elements of historical heritage. This methodology is based on the development of an inverse characterization model of the thermal response of the heritage elements in a known state of conservation through standard monitoring. The use of standard monitoring will facilitate its obtaining and its remote control. The selected input variables are easily obtainable guarantees the integration of the proposal in any typology of heritage elements. For these reasons, the main aim of this paper is to develop a complementary conservation method for historic heritage elements. This method is based on a thermal baseline model. This model is obtained by inverse thermal techniques through experimental data of the element. Once the model is identified, the model serves as a reference for the comparison between the real-time measurements of the thermal conditions of the well's surface and the surrounding microclimate. This comparison was able to create alarms for the asset manager to communicate the need for an "on-site" inspection of the item. The proposed method does not replace the current conservation mechanisms, but because of its low cost and ease of implementation, it provides a solution to the lack of monitoring of the state of conservation of historic heritage elements.

2 Method

The core of this methodology is defined and validated as a procedure to develop a baseline model. This model is used to estimate the thermal response of cultural elements to weather excitations in reference conditions. Reference conditions are defined by the personnel responsible for the maintenance of the property and refer to an optimal state of conservation. Conservation state that is considered a reference for this inverse characterization to be performed. The identification of the model requires sensors for air temperature, surface temperature, radiation, and humidity. These variables allow knowing the response of the elements and characterizing the climatic excitations of their environment (Gallego-Cartagena et al., 2020). These sensors will be fixed to the asset and their data will be recorded electronically using GPRS technology. Then, the conservation officer will have the actual measured response of the element and the estimation made by the characterization model. This estimation should be identical with the measured value if the historical element is in the reference conditions. Since the weather variation (summer, winter etc...) is considered by the developed mathematical model. Therefore, the proposed procedure hypothesizes that the differences between the measured and estimated value are due to changes in the state of conservation of the property. This difference becomes the key performance indicator that allows conservation personnel to establish the need for a visual inspection of the real state of conservation (Gómez-Plata et al., 2019; Murillo A. et al., 2020).

Hence, the proposed methodology can serve as a method of continuous monitoring and conservation management. Also, it is a low-cost and agile solution that allows the creation of distance control. It let to be replicated in all historical elements that are managed by the same institution. For example, the number of elements in Granada is greater than a million.

The methodology applied in this work to achieve the objectives is outlined in Figure 1.

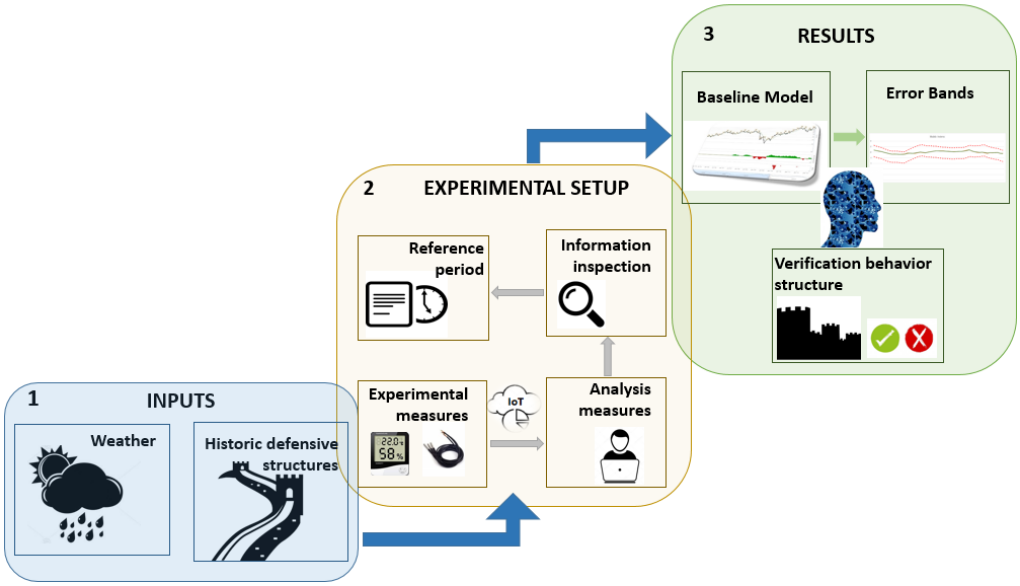

Figure 1. Overview of the three steps of the methodology

The first step of methodology (see Figure 1) is analysing of historical elements: state of conservation and weather conditions. The required climatic conditions are dry air temperature, relative humidity, and incident radiation (global and direct). In turn, the state of conservation of the element can be done as it appears in the literature in works such as that of Silva et al. (Silva et al., 2020d). The result of this step is the definition of reference conditions: the initial state of the cultural heritage elements and climatic excitations. If the state of conservation is not correct, you should first carry out an intervention to improve it. These interventions could be physical cleaning, chemical treatments to eliminate deposited particles or growth of plant species, among others. This happens with the case study shown in section 4. Also, model inputs include local climate parameters and comprehensive information on the historic heritage element. Any restoration, as appropriate, must have been performed before launching the procedure. Since the proposed mathematical model will estimate the thermal response of the element under these reference conditions (step 2 in Figure 1). If differences appear between the measured values and the model estimates under reference conditions (step 3 in Figure 1), it can be said that something is happening to the element.

The second step of Figure 1 contains actions to define the required monitoring, its installation, analysis and verification of measurements and communications. But above all, the establishment of the measured values that constitute the reference situation. These measures values are used to calibrate the baseline model and to establish a reference period in which the heritage element is in optimal condition (reference conditions). The period should be defined to cover seasonal variations, at least summer and winter. The reference period data are used to build the baseline model, subsequently applied to estimate the thermal response for comparison to the readings recorded over time. Consequently, the evaluation of the quality of the measured data and the obtaining of the model coefficients are obtained during stage 2. This stage 2 concludes when the baseline model has been validated. For this, a different sample of experimental data from the one used for the identification of the model must be used and validated both in winter and in summer due to the possible variation in climatic conditions, especially radiation.

Finally, the model for the historic heritage element in reference conditions is available, it is possible to compare the model estimation of surface temperatures under the measured excitations in real-time and the measured value of surface temperatures. That comparison (step 3 in Figure

1), based on error bands, delivers the diagnosis on which a maintenance protocol for this type of structures can be designed. Where the measurements lie within the reference range the heritage element is deemed to be in good condition. If anomalies are detected, the system alerts to the need for on-site inspection. That is, the personnel in charge of the conservation of these elements must review the differences obtained between the measured value and the one estimated by the model. And they should decide when to carry out an "in situ" inspection of the element. But, the results of this paper provide an easy-to-implement, low-cost methodology for rapid detection. And above all, it facilitates the work of conservation entities. Just like previous authors (Gredilla et al., 2019; Islam et al., 2019; Ramírez et al., 2020, 2019; Rojas et al., 2019; Saikia et al., 2018; Wilcox et al., 2015), the methodology used will assist in future strategies for the evaluation and recovery of important constructions exposed to climate change and atmospheric pollution. Therefore stage 3 consists of the implementation of the baseline together with the error band in a management system. An example of the application of this step is described in section 4.5.

In this case of this paper, the element is a historical defensive structure. However, the method can be applied to a multitude of types of elements. In this work, it has been decided to work on the historical defensive structures due to the high level of neglect in which they are found, at least in the case of Granada. There are more details about the validation case in section 4. Also, section 3 develops the theoretical foundations of the model, as well as the main hypotheses established. Finally, discussion of the work carried out in section 5 and the main conclusions obtained in section 6 are exposed.

3 Theory

3.1 Baseline model fundamentals

As noted, the procedure proposed requires a model for the thermal characterisation of defensive structures based on their orientation, geometry, and surrounds, as well as surface temperature and other features of the local climate. A review of the literature failed to identify a single inverse characterisation model (i.e., a model in which the parameters are obtained empirically) designed to that purpose. Studies on building enclosures that can be extrapolated to such structures have been described, however. The main advantages of the most common approach in physical modelling based on differential equations include simplicity and ready comprehensibility, although they call for information on a series of very complex parameters identified from empirical measurements. Figure 2 depicts the concept on which the proposed baseline is based.

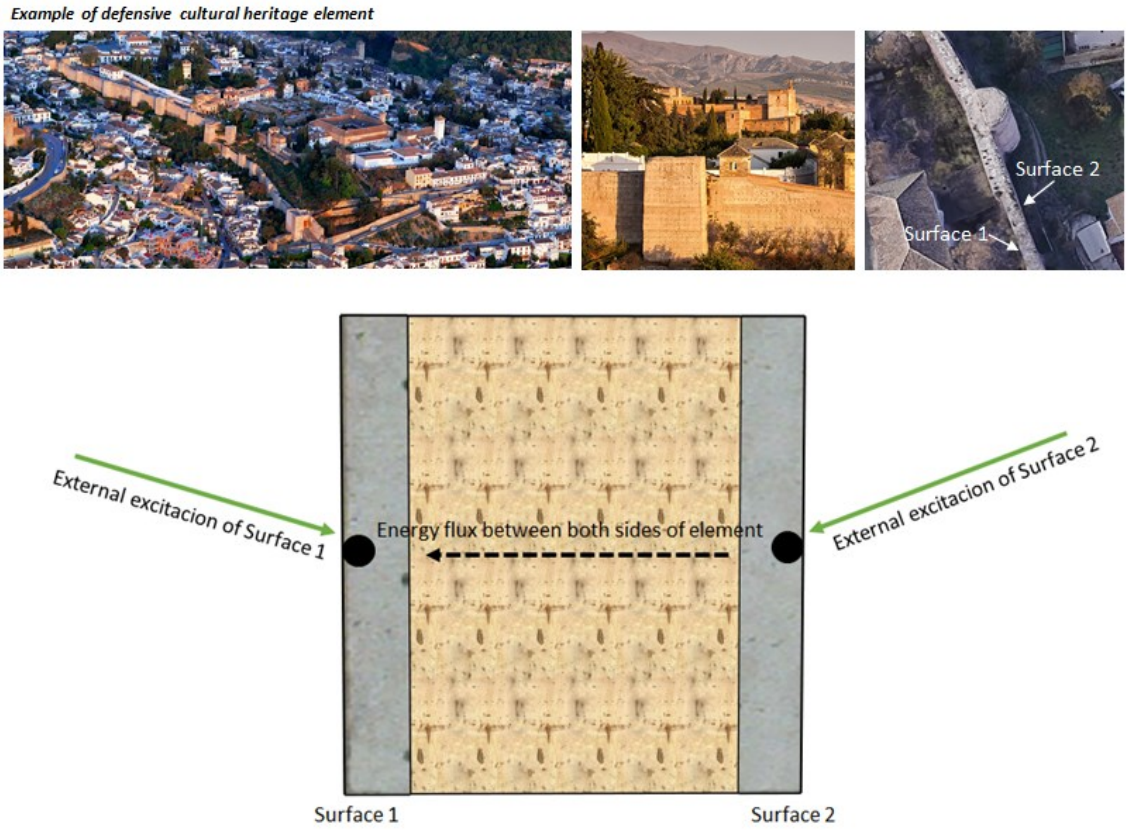

Figure 2. Standard thermal excitation in defensive structures

External excitation of surface 1 and 2 in Figure 2 are the effects of air convection, solar irradiation, and longwave radiation exchange with surroundings in the asset. Assuming the variable measured to be the surface temperature on both sides of the structure, the model should be built around that parameter. That entails drawing up an energy balance on each side of the heritage element (Eq. 1 and 2) and assuming that the temperatures measured on each surface (T_1 and T_2) are representative of the temperature of a fraction of the mass of the element. Eq. 1 and 2 are transient energy balance consider a surface element as a capacity system (Bergman and Incropera, 2011)

$$m_1 \cdot cp \cdot dT_1/dt = Q_{SE-1} - Q_{CV-1} - Q_{RD-1} - Q_{CD} \quad \text{Eq. 1}$$

$$m_2 \cdot cp \cdot dT_2/dt = Q_{SE-2} - Q_{CV-2} - Q_{RD-2} + Q_{CD} \quad \text{Eq. 2}$$

where m_1 and m_2 (kg/m^2) are enclosure surface density; and Cp (J/kg·K) is the specific heat defined in keeping with the composition of the element. Eq. 1 and 2 shows the variation of the temperature of the surface layer of the element as a function of the different heat fluxes that are present in environmental conditions. Each of them will be described in the following lines. Each of the heat fluxes present in equations 1 and 2 have been modelled taking the basic hypotheses of calculating heat transfer by conduction, convection, and radiation phenomena. These hypotheses have been assumed because they are present in most of the specialized books on the subject (Bergman and Incropera, 2011; Çengel Afshin J, n.d.; Lienhard and Lienhard, 2011)

The solar heat absorbed, Q_{SE} ($Q_{SE-1}$and Q_{SE-2} in eq. 1 and 2), is defined in Equation 3:

$$Q_{SE-i} = \alpha_i \cdot I_{RR-i} \quad \text{Eq. 3}$$

where α_i is absorptivity of the surface i studied and I_{RR} (W/m^2) the incident radiation, taking heritage element and surrounding object shading into account.

Heat convection, Q_{CV} ($Q_{CV-1}$and Q_{CV-2} in eq. 1 and 2) on each surface is defined as in Equation 4:

$$Q_{CV-i} = h_{CV-i} \cdot (T_{AIR} - T_i) \quad \text{Eq. 4}$$

where h_{CV-i} (W/K·m^2), the heat convection coefficient may vary on the two sides of the heritage element, whereas the outdoor air temperature, T_{AIR}, is the representative temperature of the air. T_i is the temperature of the studied surface (T_1 or T_2). The main hypothesis considered is that the convective transfer coefficient is very stable and can be considered invariant.

Q_{RD} ($Q_{RD-1}$and Q_{RD-2} in eq. 1 and 2), longwave radiation exchange is defined as in Equation 5:

$$Q_{RD-i} = h_{RD-i} \cdot (T_{RD} - T_i) \quad \text{Eq. 5}$$

where T_{RD} (K), the mean radiant temperature assuming a form factor of 0.5, is defined in terms of the sky temperature T_{SKY} (K) and the ground or adjacent surface temperature T_{AIR}, assumed to be the same as the temperature of the surrounding air. Mean radiant temperature is found with Equation 6 and the radiation coefficient, h_{RD-i} (W/K·m^2), with Equation 7.

$$T_{RD} = T_{AIR} + T_{SKY}/2 \quad \text{Eq. 6}$$

$$h_{RD-i} = 4 \cdot \sigma \cdot \varepsilon_i \cdot ((T_{RD} + T_i)/2)^3 \quad \text{Eq. 7}$$

where σ, the Stefan-Bolzman constant, adopts a value of $5.67 \cdot 10^{-7}$ W/m^2·K^4 ε_i and ε_i is the surface's longwave emittance. It is assumed that the radiant exchange can be linearized since the error made is lower than 3% (Çengel Afshin J, n.d.).

Heat conduction, Q_{CD} *in* eq. 1 and 2, between the two surfaces is found with Equation 8:

$$Q_{CD} = k \cdot (T_1 - T_2)/L \quad \text{Eq. 8}$$

where L (m) is the wall thickness and k mean thermal conductivity (W/m·K).

The described system of equations (1 through 8) describes a physical model of the heritage element. Finding the parameters involved (convection coefficient, absorbance) from measured data calls for complex and variable calculation. The model was therefore re-structured in terms of transfer functions (Díaz et al., 2018; Stephenson and Mitalas, 1971), as shown in Equations 9 and 10:

$$T_1(t) = \sum_{i=0}^{m} a_i \cdot T_2(t-i) + \sum_{i=o}^{m} b_i \cdot Texc_1(t-i) + \sum_{i=1}^{n} d_i \cdot T_1(t-i) \quad \text{Eq. 9}$$

$$T_2(t) = \sum_{i=0}^{m} aa_i \cdot T_1(t-i) + \sum_{i=o}^{m} bb_i \cdot Texc_2(t-i) + \sum_{i=1}^{n} dd_i \cdot T_2(t-i) \quad \text{Eq. 10}$$

where $T_1(t)$ is the temperature of one of the surfaces, $T_2(t)$ the temperature of the other and $T_{exci}(t)$ an equivalent temperature referred to the radiant and convective excitations to which each surface is exposed. Two surfaces have been taken to show the theoretical foundations of the baseline for a certain asset. In the other hand, calculation of the excitation temperature ($Texc_1$ in surface 1 and $Texc_2$ in surface 2) is described in the following section.

The model coefficients, which refer to the physical parameters in Equations 1 and 2, are assumed to be invariable over time. Coefficients a_i and b_i are associated with temperature model 1, and aa_i, and bb_i with model 2 excitations. Coefficients di and dd_i denote model dependence on its prior response (earlier time intervals) due to system inertia.

As Equations 9 and 10 show, finding the surface temperature on one side depends on the temperature found for the other. The two expressions are consequently interlinked and must be solved as a system of equations with two unknowns.

The model is dynamic not only because of the nature of the input excitations but also of its dependence on the prior response elicited by the target variable. The number of prior time intervals is optimised for each specific system.

The assumptions embedded in the model are listed below.

- As the target variable varies widely throughout the day, the hour is the optimal time interval and step-time.
- Given the use of constant coefficients and concomitant model invariance, separate models are initially deemed to be required for summer and winter to accommodate climate differences.
- While implicit in the thermal capacity of the enclosure and the surface temperatures, the effect of indoor relative humidity is stable over time.
- The model coefficients defined for a given reference period establish the model's best fit for that period.

The section below describes the calculations proposed to find the equivalent excitation temperature and the respective coefficients.

3.2 Thermal excitation

As explained earlier, outdoor excitations include convection heat exchange with the surrounding air, solar radiation absorbed and longwave radiation exchange. The equivalent temperature defined in Equation 11 encompasses all three:

$$T_{EXCi}(t) = \frac{h_{CV-i}(t)\cdot T_{AIR}(t)+h_{RD-i}(t)\cdot T_{RD(t)}}{h_{CV-i}(t)+h_{RD-i}(t)} + \frac{\alpha_i}{h_{CV-i}(t)+h_{RD-i}(t)} \cdot I_{RR-i}(t) \qquad \text{Eq. 11}$$

Calculating the excitation temperature of each surface entails working with the unknown variables discussed above, which can also be estimated from coefficients b_i and bb_i in Equations 9 and 10 more readily, for they correct the parameter values.

The values adopted were as follows.

- Further to Kirchoff's law, a single value was used for emissivity and absorptivity for the surfaces involved. The Lienhard et al. (Lienhard and Lienhard, 2011) approximations for these complex functions of temperature, angle and wavelength are generally agreed to be reasonable.
- Convection transfer coefficient $h_{cv\text{-}i}$ was calculated in terms of incident wind velocity using the McAdams correlation (McAdams W, 1958), a solution frequently resorted to in the literature (Malgorzata et al. (O'Grady et al., 2017)).
- Radiant transfer coefficient h_{RD} was calculated as per Equation 7.

In another vein, the incident radiation on each surface calls for basic solar calculations, for the parameter used is direct and diffuse incident radiation on a horizontal plane. As those calculations are routine in solar technology assessments, the literature was reviewed, and the following conclusions are drawn.

- The sun's position (solar height and azimuth) can be estimated from a heritage element's location and the time of day (Hafez et al., 2018, 2017).
- The instantaneous incident radiation on the surface studied is found by projecting the radiation measured using solar direction and surface cosines (Fernández-Ahumada et al., 2017; Hafez et al., 2018; Skouri et al., 2016).

Sky temperature is cited as an obstacle in all the papers reviewed. In some, such as (Maghrabi and Clay, 2011), it was estimated experimentally, although it was most commonly found with tested empirical models (Antonanzas-Torres et al., 2019; Evangelisti et al., 2019). The Aubinet model (Aubinet, 1994), one of the most widely extended according to the preceding two references, calculates sky temperature from Equations 12, 13 and 14.

$$T_{Sky} = \varepsilon_{SKY}^{0.25} \cdot (T_{AIR} + 273.15) - 273.15 \quad \text{Eq. 12}$$

Sky emissivity ε_{SKY}, was found with Equation 13:

$$\varepsilon_{SKY} = F_{Cloudiness} \cdot (0.787 + 0.764ln\left(\frac{T_{DEW}+273.15}{273.15}\right) \quad \text{Eq. 13}$$

where the dew-point temperature was calculated with the ASHRAE correlations (Ashrae, 1997) for relative humidity and dry bulb temperature. $F_{Cloudiness}$, the cloudiness factor, was defined as in Equation 14:

$$F_{Cloudiness} = 1 + 0.024E_N - 0.0035\left(E_N{}^2\right) + 0.00028(E_N{}^3) \quad \text{Eq. 14}$$

where E_N, cloudiness, was assumed to be a constant, with a value of 3 in summer and 5 in winter.

Hence, all the model's independent variables could be estimated in terms of two excitation temperatures, T_{EXC1} and T_{EXC2} (Equation 11).

3.3 Model characterisation

The values for the model coefficients were found as follows.

1. The number of coefficients associated with system inertia was chosen (d_i and dd_i in Equations 9 and 10) in keeping with the expected time constants and the step-time defined in the model. It was defined as 1 (low thermal capacity or walls less than 0.5 m thick), 2 (standard value for walls less than 2 m thick) or 3 (walls with high thermal capacity or over 3 m thick) for a step-time of 1 h, on the grounds of findings reported by Giuseppina et al. (Ciulla et al., 2010), who made the number of poles in the transfer function dependent upon the main constant in the system to be characterised.
2. The number of excitation-related (a_i, b_i, aa_i and bb_i in Equations 9 and 10) and system inertia-related coefficients were established, along with one random coefficient.
3. Coefficient values were determined on a sub-sample of the experimental data gathered during the reference period, in which the following requisites had to be met:
    - Acceptable minimum square error
    - Consistency of the signs adopted by the coefficients with the nature of the excitation and the value of the respective steady-state.

    If one of those two requisites was not met, item 2 above was repeated with a larger number of numerators and the result compared to the preceding trial.

The models so characterised were then implemented, as shown in Figure 3.

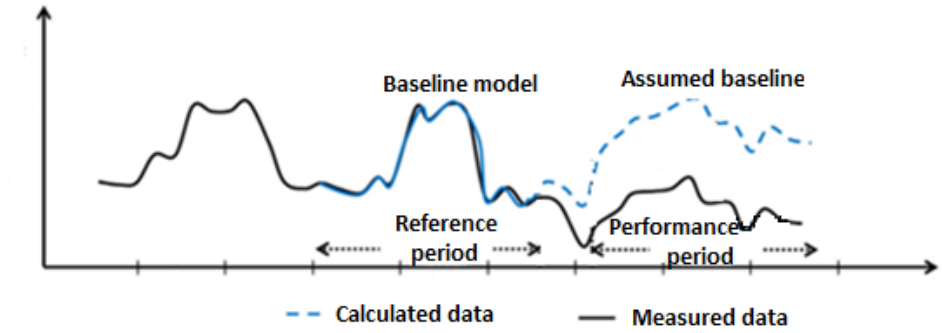

Figure 3. Example of a baseline model

Since the model was built and subsequently applied using experimental data, the uncertainty associated with both it and the measured data was analysed. This uncertainty is estimated using the Taylor series in eq. 15 and 16 (Coleman and Steele, 2018). Radiation and temperature were the main model variables dependent upon measuring instruments. Although relative humidity was also used, as it was confined to intermediate calculations the respective uncertainty was disregarded. The standard deviations for the variables, governed by the respective measuring instruments and included in the model were calculated since eq. 15:

$$Err_{T1} = \left|\frac{\partial T_1(t)}{\partial T_{out}}\right| \cdot \sigma(T_{out}) + \left|\frac{\partial T_1(t)}{\partial T_1}\right| \cdot \sigma(T_1) + \left|\frac{\partial T_1(t)}{\partial Irr}\right| \cdot \sigma(Irr) + \left|\frac{\partial T_1(t)}{\partial T_2}\right| \cdot \sigma(T_2) \quad \text{Eq. 15}$$

$$Err_{T2} = \left|\frac{\partial T_2(t)}{\partial T_{out}}\right| \cdot \sigma(T_{out}) + \left|\frac{\partial T_2(t)}{\partial T_1}\right| \cdot \sigma(T_1) + \left|\frac{\partial T_2(t)}{\partial Irr}\right| \cdot \sigma(Irr) + \left|\frac{\partial T_2(t)}{\partial T_2}\right| \cdot \sigma(T_2) \quad \text{Eq. 16}$$

where:

- $\sigma(T_{out})$, is the sensor-related standard deviation for outdoor temperature
- $\sigma(T_1)$ and $\sigma(T_2)$, are the standard deviations for (likewise sensor-related) surface temperature
- $\sigma(Irr)$, the standard deviation for radiation, was not a direct measurement but processed from the readings recorded and found to be 50 W/m$^{2.}$

Error bandwidth was calculated as follows:

$$T_{1-estimated}(t) = T_1(t) \pm Err_{T1} \quad \text{Eq. 17}$$

$$T_{2-estimated}(t) = T_2(t) \pm Err_{T2} \quad \text{Eq. 18}$$

The method ultimately delivered an estimate of the expected surface temperature and the band defining acceptable deviation. Readings outside that band were deemed to be anomalous and their accumulation an indication of the need to ascertain the condition of the heritage element. The following section describes a case study in which the methodology was applied.

4 Case study: results

4.1 Description of case study

The heritage element chosen was a section of the Zirid Wall around Cadima Citadel (Figure 4) in the city of Granada. The wall surrounds San Nicolás Hill, enclosing an area of about 75 hectares. The main part of the wall still standing stretches for 390 m along the northern flank. This section houses the *bāb Qaštar* gate, better known as San Cecilio Chapel. One of the oldest surviving elements, little is known about its initial form or any subsequent renovation. This element has

been chosen due to the challenge of validating the proposed methodology in a structure within an urban area at risk due to anthropogenic agents and the growth of the city.

Figure 4. Case study: Zirid Wall, Granada. Source: PREFORTI Project and own development from Google Earth

Granada is a city of enormous cultural value (Oliveira et al., 2019a), hence the interest of the authorities in having a preventive conservation methodology. Zirid wall was chosen because its degradation has accelerated in recent years and it was challenging to demonstrate the usefulness of the procedure here.

In the rammed earth technique used to build it, widespread in eleventh to fourteenth-century construction, walls were erected by pounding soil into a mould consisting in two parallel, vertically positioned boards spaced to the intended width of the wall and held together with crossbars. The resulting box was then filled, lift-by-lift, with rammed soil or lime mortar. In the case studied here, two construction techniques were deployed: concrete- and lime mortar-rendered rammed earth, both depicted in Figure 5. These data are known because a detailed study has been made of the current situation of the property and a series of tastings to find out its composition. The methodology does not require knowledge of these data. However, they show that the interior composition of elements with hundreds of years of existence is a variable full of uncertainty and difficult to obtain.

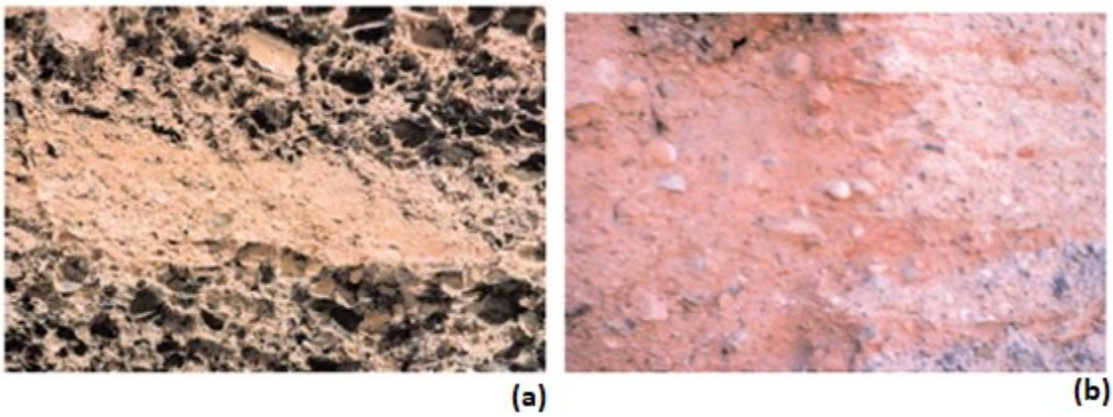

Figure 5. Composition of the wall studied: concrete (a) and lime mortar-rendered rammed earth (b). Source: PREFORTI Project

The incident radiation had consequently to be determined on both sides, further to the methodology proposed. It is due to the different level of radiation in the function of the relative position with the sun.

This case study exemplified the utility of the methodology to diagnose historic constructions. Although much of the initial wall has disappeared, the remaining sections constitute one of the most prominent heritage elements in this part of Granada's historic neighbourhood. The structure is listed as a cultural heritage element, the highest level of protection envisaged in Spanish legislation (Estado, 1985), and lies in a quarter accorded UNESCO World Heritage Site status in 1994. Its preventive conservation would be favoured by the diagnosis and verification method proposed here.

The condition of the various sections of the Cadima Citadel wall varies. In some, the full width of the original structure is in nearly perfect condition, whereas in others it has disappeared altogether or remains as a mere archaeological token. Those differences are due primarily to:

- Environmental damage induced by erosion attributable to temperature gradients and frost, with concomitant intermediate or substantial mass loss; surface water runoff and leakage; wind; geomorphological-mediated cracking, detachment and structural damage including deep vertical cracks, fissures, hollowing and loss of shape; parasitic and medium-sized plant life, with surface soiling; insects, birdlife and rodents
- Anthropic action, including neglect, the disappearance of the initial use, inappropriate past restorations and lack of suitable maintenance that heightens instability and the risk of deterioration.

The studies conducted on the wall during the reference period, illustrated in Figure 6, were designed to analyse possible pathologies and formulate conservation measures or, if the wall was found to be in good condition, undertake reference period monitoring. To obtain these pathologies, thermography, composition studies, sample analysis and historical data review have been carried out.

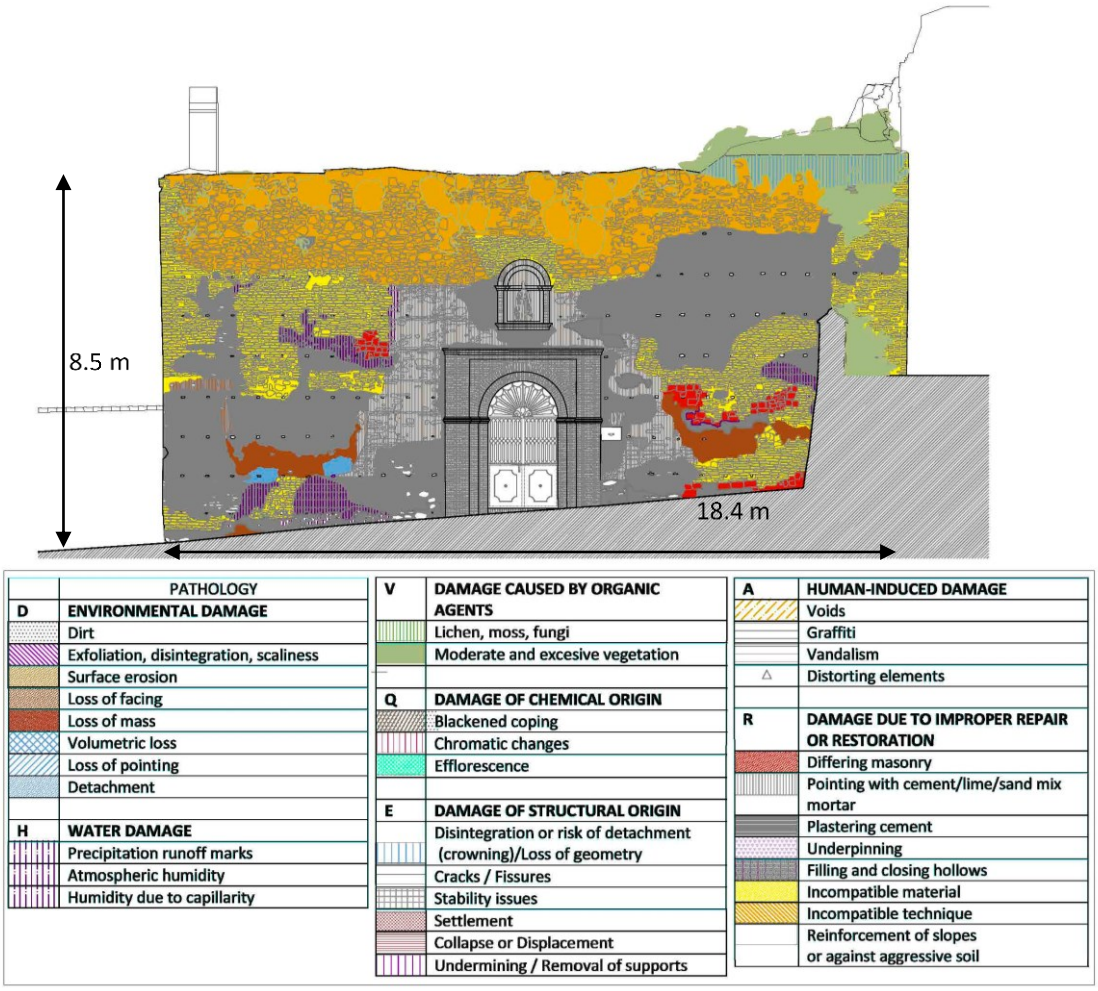

Figure 6 Pathologies detected in Zirid Wall (San Cecilio Chapel area). Source: PREFORTI Project

4.2 Experimental setup

With a view to the inverse characterisation referred to earlier, a monitoring system was designed for a representative sample of wall panels (two in the case study). The following sensors were installed:

- surface temperature sensors, one per panel, with two probes each, one for each side or surface of the panel. Sensors are contact thermocouple connected to a little data acquisition system. The data acquisition system is connected to a raspberry for sending us the experimental data. Raspberry has an internal memory too. Each surface has a representative sensor of its temperature and it would be the witness sensor that must be left installed in the property for remote management. Sensors are PT100 which achieves an accuracy ± 0.01 °C ± 1 digit
- environmental temperature and relative humidity sensors to record the conditions in each of the microclimates extant in the areas studied. The NTC thermistors are located inside a Testo 174 T data logger with an accuracy of ± 0.2 °C. These environmental temperature dataloggers set inside 80 mm diameter, 50 cm long cylindrical tubes with an outer reflective cover in the lower two-thirds housing the probe and uncovered in the black upper third to generate movement induced by natural convection to obtain a

representative ambient temperature value (see Figure 7), installed to ensure that the readings recorded were sufficiently accurate for the study

- Weather station to measure the local weather, primarily radiation for want of specific sensors for that parameter, which proved to be one of the determinants for developing the performance model. These outdoor conditions data were recorded on a Weather Station WatchDog 2000, installed on top of the house as shown in Figure 9.

Figure 7. Sensors for monitoring outdoor temperature. Source: J. Arco

The complete system has a battery with an estimated life of 24 months. Although it can be powered by solar energy. The memory of the system is greater than 5 years with a data log every 10 minutes.

All the instruments were positioned with utmost care to ensure that the attachment systems would not damage the surface to which they were secured, given the wall's architectural and heritage value. The panels studied are outlined in the photograph in Figure 8: panel 1 (which houses the main gate) in red and panel 2 (at the rear) in yellow.

Figure 8. Defensive structures studied. Source: Own development from Google Earth

Figure 9, in turn, shows the position of the sensors. Panel 1, comprising one of the main and largest sections of the wall, was instrumented with two surface temperature sensors, one on the main wall (TT1-1) and the other (TT1-2) which, given its proximity was deemed to have established connectivity with panel 2; along with two temperature and relative humidity sensors (TH1-1, TH1-2) and one datalogger. Similarly, panel 2 was fitted with two surface temperature sensors (TT2-1, TT2-2) on its two orientations and one temperature and humidity sensor (TH2). As monitoring was conducted with all the sensors from August 2018 to January 2019, inclusive, it covered both winter and summer months. Also, the weather station records dry air temperature, relative humidity, wind speed and direction, global horizontal radiation, and direct radiation.

Figure 9. Sensor positioning. Source: own development from Google Earth

4.3 Empirical data

This section describes the experimental data gathered, in which together with the outdoor variables, particular attention was paid to the accuracy of the surface temperatures, the target variable.

By way of example, the readings recorded in different periods by one of the surface temperature sensors on each panel studied are analysed below, along with the effect on the values of different weather conditions. For this, the effect of incident radiation on surfaces during summer and winter will be analysed.

The readings for panel 1 and more specifically for sensor TT1-1 (representative sensor for panel 1) are shown in Figure 10. As the graph shows, the temperature was essentially the same on the two surfaces and closely related to the air temperature near these surfaces (TH1. It is obtained as an average between TH1-1 and TH1-2). Nonetheless, the surface temperature of surface 1-2(sensor TT2-1), which in the model referred to the temperature on the rear surface, were consistently higher, suggesting that incident radiation affected that area due both to orientation and shading. The incident radiation values are plotted for the two surfaces in Figure 11.

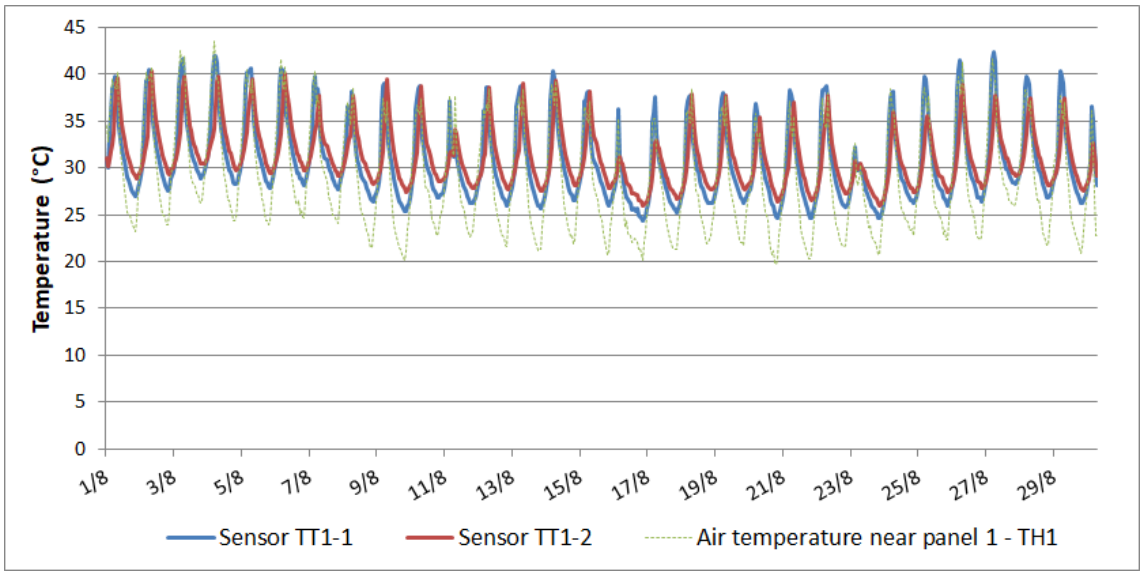

Figure 10. Experimental data during summer in panel 1: surface temperature on the front (TT1-1), rear surfaces (TT1-2) and air temperature (TH1).

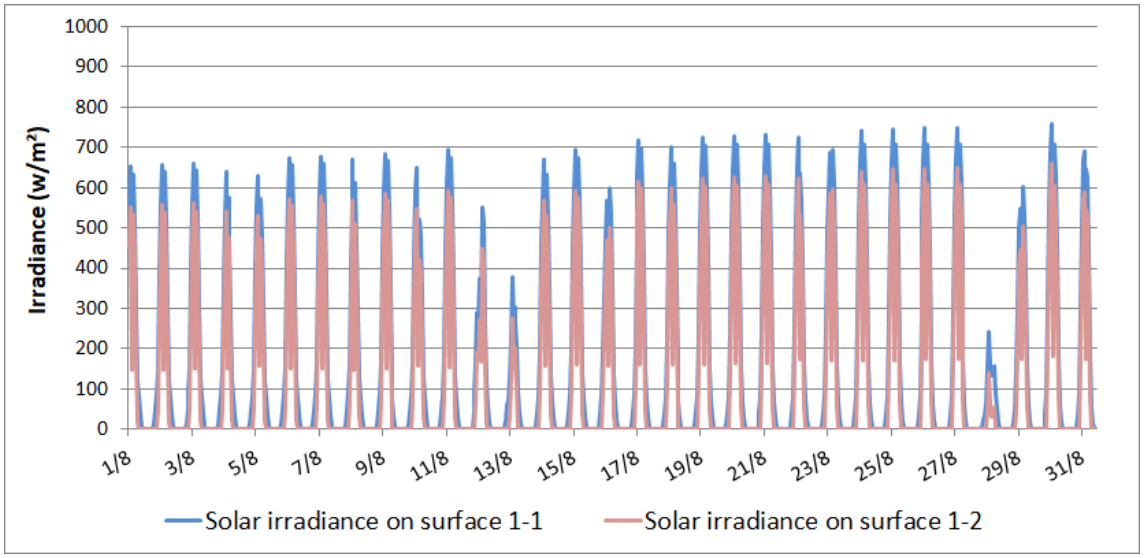

Figure 11. Incident radiation on the front and rear surfaces of panes 1in summer

The experimental data attested to the need to include both outdoor temperatures and incident radiation in the model.

Pan analogous analysis was conducted for panel 2, focusing on sensor TT2-1. As Figure 12 shows, the differences between the two surfaces of panel 2 were wider during winter. It is selected winter to show the effect of solar irradiance.

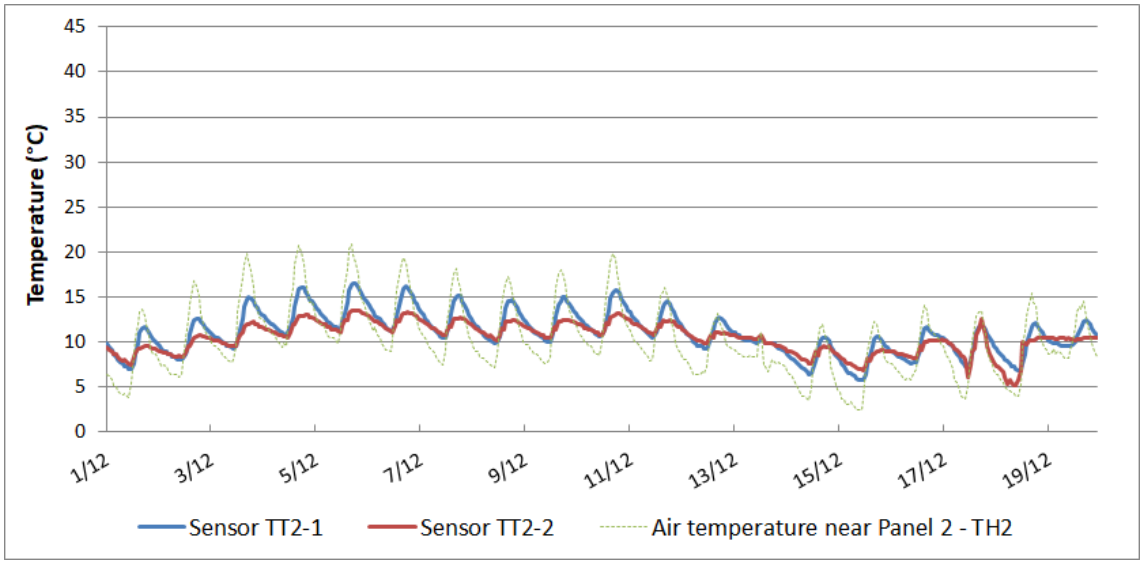

Figure 12. Experimental data during winter in panel 2: surface temperature on the front (TT2-1), rear surfaces (TT2-2) and air temperature (TH2).

The comparison between the air temperature near of panel 2 (see TH2 in figure 12) and surface temperatures (TT2-1 and TT2-2) depicted in Figure 12 shows that the near match observed in Figure 10 was absent in this case. The difference may be attributed to the variation in incident radiation on the surfaces, graphed in Figure 13.

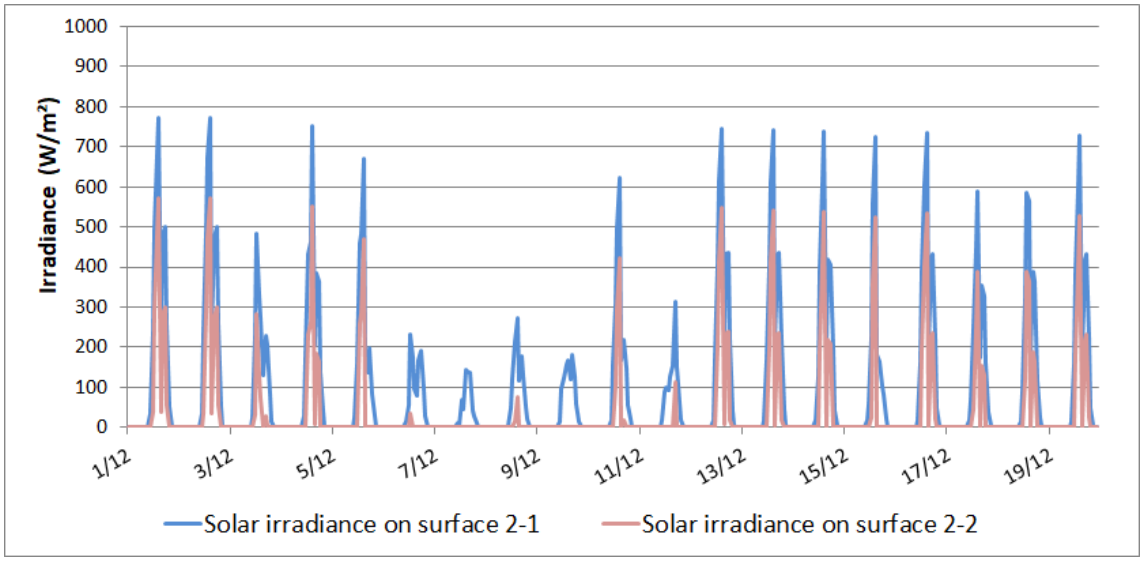

Figure 13. Incident radiation on the front and rear surfaces of panel 2 in winter

The fluctuation in surface temperature with the surrounding environmental conditions exhibited similar behaviour. The model proposed accommodates the outdoor conditions impacting the

wall.and the thermal inertia of the wall itself, associated with its construction. The building techniques are implicit in the mathematical formulation described in section 3.1.

The above results highlight the need for the proposed model to respond to the physics of the phenomenon. Having a model for the representative temperature of the well in the chosen control surface. This model must be identified with a winter and summer period and validated with different experimental data. In this way, it is ensured that the range of applicability of the same will cover all the annual climatic variation to which it is subjected. In the next section, the TT2-1 sensor is taken to show the importance of the reference period for obtaining the model coefficients. This reference period should contain data for summer and winter as the climatic excitations are different. This mixture of data guarantees a greater range of applicability of the model. However, the model allows it to be identified during winter and executed in summer or vice versa, and guarantee acceptable results. This conclusion is tested in the next section.

It should be noted that the application of the proposed methodology requires the choice of reference points of cultural heritage element. At these points, a surface temperature sensor and coincident weather conditions must be installed. To increase the replicability of the procedure, it works with the minimum number of monitoring points, although the ideal is to choose surfaces that have different excitations, different surface treatments or different states of conservation.

4.4 Baseline model

The data of TT2-1 were divided into four groups to determine the coefficients for this model. The first contained data measured in the warm season from August to October, and the second in the cold season from November to January. Each group was subdivided into two datasets of approximately the same size, one used for model fitting and the other for validation. November was deemed to be the transition month between summer and winter.

The surface temperatures calculated with the model for the warm season are plotted against the experimental data in Figure 14, which attests to a very close matching, confirmed by the error values set out in Table 1.

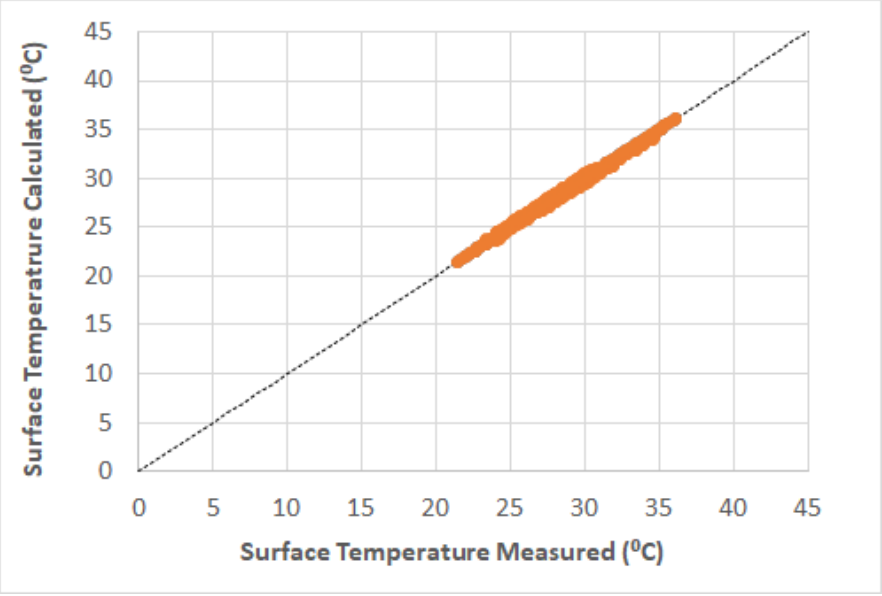

Figure 14. Summer model data versus experimental readings

An analogous procedure deployed to characterise the model for cold season data yielded the graph depicted in Figure 15, where the validation dataset was plotted against the model estimates. The match found was even closer.

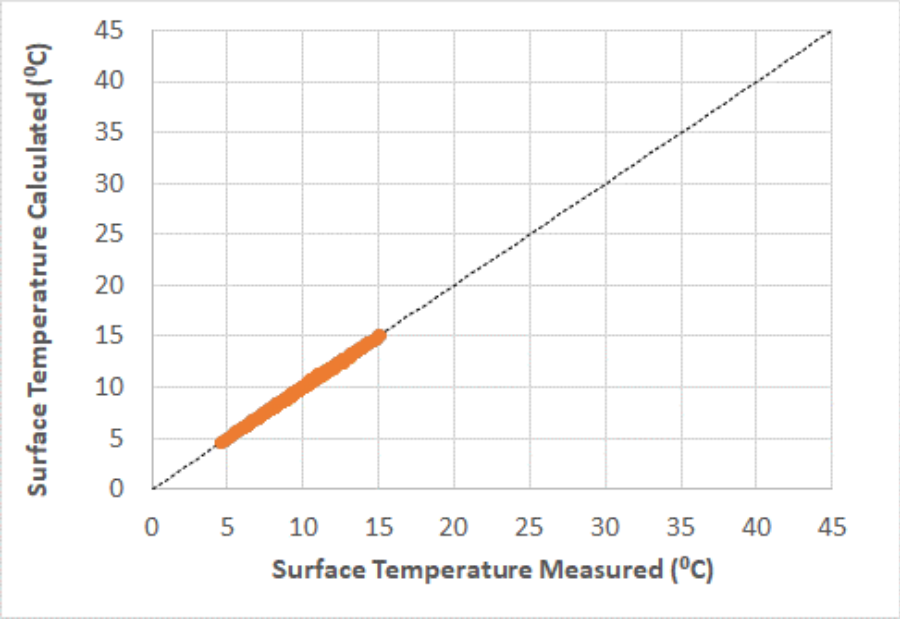

Figure 15. Winter model data versus experimental readings

Figures 14 and 15 attest to model reliability in both cases and despite the variations observed, to a certain relationship between them. On those grounds, the use of a single model for summer and winter was envisaged, in which the differences in excitation in the two seasons would be accounted for in the input variables for this physical model. That possibility was tested for the various combinations with the results given in Table 1.

Table 1. Maximum and mean absolute errors for winter and summer models applied to both seasons

Reference period	**Period applied**	**Maximum absolute error**	**Mean absolute error**
Winter	Winter	2.89	0.82
	Summer	3.51	0.95
Summer	Winter	3.38	0.79
	Summer	2.75	0.72

As the values determined showed no significant differences between the two models, either one of the two could be applied throughout the year. The summer model was ultimately chosen, for it yielded lower maximum and mean absolute errors. Moreover, the input excitations varied more widely in the summer model due to the characteristics of the local climate. Therefore, what was previously ventured is confirmed: the physical parameterization of the model allows its extrapolation to climatic conditions different from those used in obtaining the model coefficients.

The baseline model established was consequently applicable to structures with different behaviour both during the day and throughout the year. Its mathematical expression involved three excitation-related and two inertia-related coefficients. The correlation coefficient, R^2, was 0.99975.

4.5 Validation and application

As noted earlier, the baseline method proposed is a model that uses information on environmental conditions, specifically outdoor temperature, relative humidity, and incident radiation to estimate surface temperature.

Since all the input variables were monitored in this study, panels of the wall other than those used to define the model could be used to validate it. As Figure 16 shows, sensor TT2-2 was analysed in a winter period different than the model reference period (using the summer model). The two curves exhibited very similar behaviour with the model able to change pattern in keeping with the experimental data. Its accurate characterisation of wave amplitude and phase differences indicated that system inertia behaved as expected.

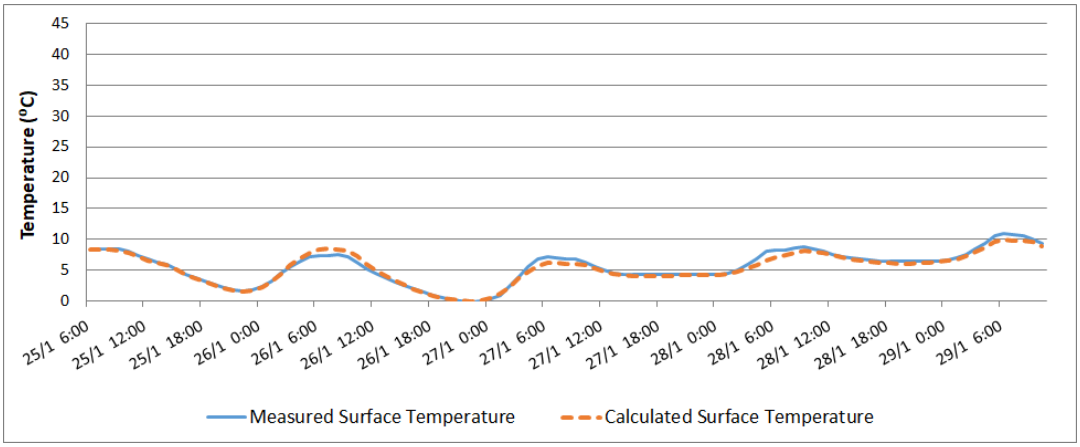

Figure 16. Validation of model at TT2-2

It is important to highlight that the results shown in the figure are the application of the identified model (calculation of coefficients) using the data from TT2-1 and executed with the excitations suffered by the surface measured by TT2-2. The good prediction of the baseline is due to the physical component of the model, which shows how the model responds with quality to different incident radiation. Furthermore, the model has been identified with summer data, and the application of the same with winter data is shown in Figure 16. The same procedure deployed with another sensor, TT2-1, for the summer, delivered the curves graphed in Figure 17.

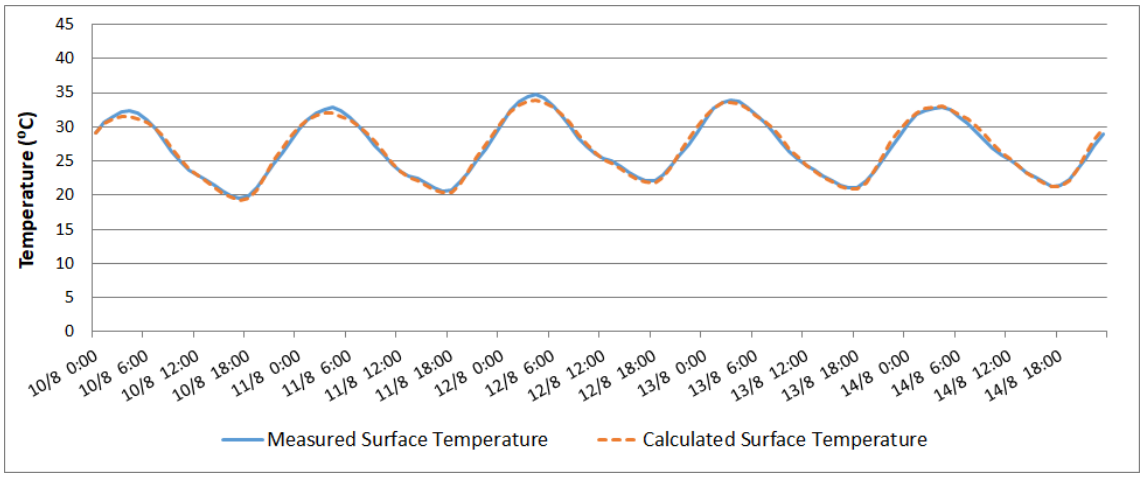

Figure 17. Validation of model at TT2-1

The baseline model developed consequently performed to expectations, reflecting the physics of the structures analysed. Moreover, as a dynamic model, it accommodated more than just the input variables for a given time. It was also impacted by prior developments on the surface analysed, as well as by those existing and existing previously in the rear surface since the model inputs include the readings for both panels.

Since the model was built and subsequently applied using experimental data, the uncertainty associated with both it and the data measured was analysed. The Taylor series method was used, as discussed in section 3.4, taking the uncertainties associated with the measurements to be 0.05 for outdoor temperature $\sigma(T_{out})$ and surface temperature $\sigma(T_1)$ - $\sigma(T_2)$

The resulting bands were subsequently applied to the baseline model defined (see Figure 18) and used to determine whether the structure behaved satisfactorily or anomalously by plotting the experimental measurements on the same graph. The proximity of some of the points recorded in the last week of August to the lower band (see Figure 18) raised the question of what might be causing that situation.

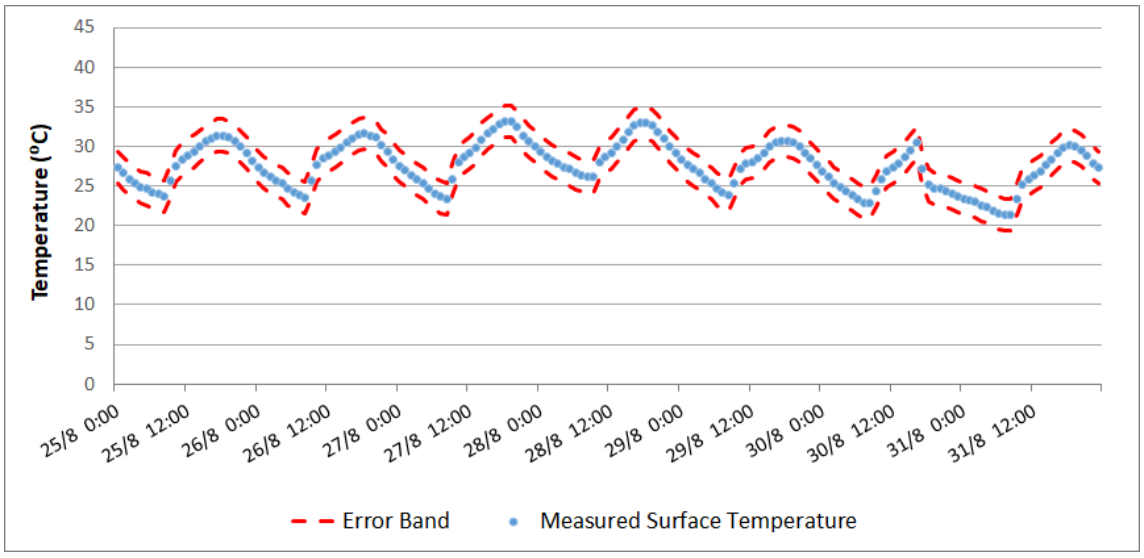

Figure 18. Baseline model error band for August

Figure 19, which graphs the data for one week in the cold season, shows that several points lay outside the error range. The inference would be an anomaly in the data measured or in the condition of the structure, which, if persistent, would call for an on-site inspection.

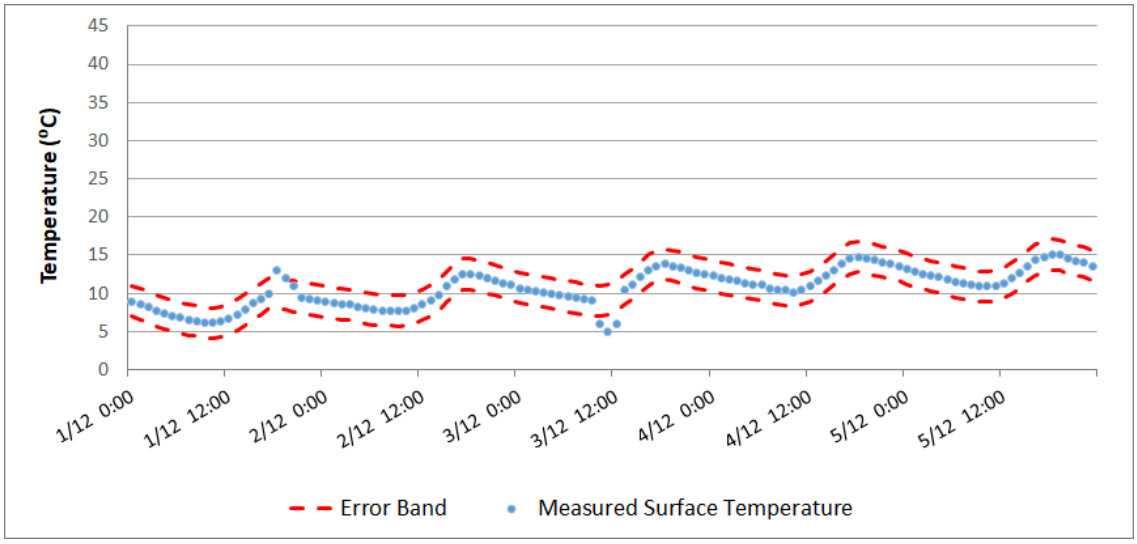

Figure 19. Baseline model error band for December

The methodology proposed generated models from differential equations. Entering temperature and relative humidity data would therefore yield information on a structure's behaviour over time and provide support for adopting preventive action decisions.

5 Discussion

The work presented proposes a preventive maintenance procedure for historical assets. This procedure is not a substitute for the need for on-site inspections but is intended to manage the frequency of that inspection. For this, a baseline model is prepared under acceptable conditions of conservation and decided by the personnel responsible for the maintenance of the property. The model will estimate the response of the good to climatic excitations and under the same anthropic demands of the reference conditions. If differences appear between these estimates and the values measured remotely, a warning will be issued to alert the personnel that the response of the good is outside the range of established reference conditions. The reason why this alarm occurs is not resolved by this work, but they need to go to the well to review it.

The procedure is easy to implement and inexpensive. It is currently being implemented by certain public institutions in support of the management office for these historical elements. The results of the application of the procedure serve to command and organize the different periodic inspections carried out by the agents in charge. It is important to note that some offices are responsible for thousands of historical elements in cities such as Rome, Granada, or Athens. Nowadays, Cultural and Historical Heritage Concierge of Andalusia is working with the researchers of this work for the implementation of this protocol. This organization is responsible for most existing cultural assets in Andalusia. They are responsible for a quantity of the conservation of millions of cultural elements but with very limited resources. The next phase of this work has begun on developing a digital platform to exploit the data recorded in a database. This database would receive in real-time the data of surface temperature and microclimatic conditions of the cultural elements on which this intervention is carried out. The server itself would implement the proposed methodology to automatically obtain the baseline. The end-user would have access to the measured values, and the comparison between the measured value and

the baseline estimate. The platform itself will have a series of notices to claim the user's attention if anomalies appear, such as those presented in section 4 results. The results of this work have generated confidence in this entity and could be replicated by other entities around the world. It should be noted that the proposed methodology serves to complement current maintenance and conservation techniques, and in no case does it replace them.

Besides, techniques as ion beam analysis, transmission electron microscopy (TEM), X-ray diffraction (DRX) and X-ray fluorescence (FRX) techniques for materials characterization and thermographic photo camera could help to get more information about historical element pathologies and composition. These techniques should be used during the initial step of methodology (see Figure 1) to analyse the real condition of the element. And it will also be required to be used if an "on-site" inspection is required due to differences between the measured and estimated value (step 3 in Figure 1).

Rather, the aim of this work is linked to a support procedure for the preventive maintenance of historical elements. But, it has a conservative hypothesis that the personal person in charge of the conservation of these assets has the necessary training and the indispensable material so that with an inspection "in situ" to evaluate the real state of conservation. For example, the cause of the proposed methodology is intended to notify staff of a possible incident on the item.

In the future, it is necessary more studies about "anthropic action" because there are a lot of influences than just "including neglect, the disappearance of the initial use, inappropriate past restorations and lack of suitable maintenance that heightens instability and the risk of deterioration" for historical elements. Anthropic actions consider atmospheric pollution by industries, the vehicular traffic, vandalism, or antique rehabilitations without registration… These actions are considered implicitly in the methodology. A change in them should be detected as an increase in the difference between the two temperatures being compared. However, its effect is of great importance in the needs of inspection and conservation of historical assets.

6 Conclusions

The methodology proposed delivers a baseline for characterising the behaviour of cultural heritage elements exposed to thermal excitation. This model supports real-time heritage element management in the form of an indicator based on real data able to anticipate the need for effective prevention.

The method was validated by application to a section of the Zirid Wall in Granada in both winter and summer and under conditions other than used to estimate the model coefficients. In percentage, the mean error values were <5%, whilst the mean absolute errors in temperature were <1ºC and the maximum absolute errors <3ºC.

The most prominent findings are listed below.

- The methodology characterises thermal inertia dynamics in structures and the surrounding environmental conditions, irrespective of their variability.
- It is readily replicable with experimental data and can be fitted with minimal and feasible monument monitoring.
- The method proposed can be used as a diagnostic tool, for it yields a reference value against which to compare experimental data and detect anomalies in an early enough phase to anticipate the need for preventive measures.

This study makes an original contribution to preventive conservation applied to historic heritage elements by enhancing the utility of routinely installed monitoring facilities. It can also be used in conjunction with tools that protect against other types of risks (seismic, pollutant agent-related) to control the condition of surviving historic elements. Finally, the procedure should be combined with the use of other techniques for field measurement of its conservation status. As well as controlling the security of the same if it can be exposed to acts of vandalism. However, this procedure will facilitate and improve their maintenance in a changing world due to climate change and possibly social and economic crises due to pandemics such as COVID-19.

7 Acknowledgements

This study was funded by the European Regional Development Fund (ERDF) under project BIA2015 69938-R (State Research Agency of Spain) 'Sustainable methodology for the conservation and maintenance of Medieval rammed-earth Fortifications in South-eastern Iberia (PREFORTI)'; and under the project 'MedEcoSuRe - Mediterranean University as Catalyst for Eco-Sustainable Renovation (A_B.4.3_0218)'.

8 References

Antonanzas-Torres, F., Urraca, R., Polo, J., Perpiñán-Lamigueiro, O., Escobar, R., 2019. Clear sky solar irradiance models: A review of seventy models. Renew. Sustain. Energy Rev. 107, 374–387. https://doi.org/https://doi.org/10.1016/j.rser.2019.02.032

Ashrae, 1997. Handbook, Fundamentals.

Aubinet, M., 1994. Longwave sky radiation parametrizations. Sol. Energy 53, 147–154. https://doi.org/http://dx.doi.org/10.1016/0038-092X(94)90475-8

Azizi, N.Z.M., Razak, A.A., Din, M.A.M., Nasir, N.M., 2016. Recurring Issues in Historic Building Conservation. Procedia - Soc. Behav. Sci. 222, 587–595. https://doi.org/10.1016/j.sbspro.2016.05.217

Bergman, T.L., Incropera, F.P., 2011. Fundamentals of heat and mass transfer. Wiley.

Bertolin, C., Loli, A., 2018. Sustainable interventions in historic buildings: A developing decision making tool. J. Cult. Herit. 34, 291–302. https://doi.org/10.1016/j.culher.2018.08.010

Bonora, A., Fabbri, K., Pretelli, M., 2019. Environmental microclimate management and risk in the unesco world heritage site of villa barbaro maser (Italy). ISPRS Ann. Photogramm. Remote Sens. Spat. Inf. Sci. 42, 269–276. https://doi.org/10.5194/isprs-Archives-XLII-2-W11-269-2019

Camuffo, D., n.d. Microclimate for cultural heritage : conservation and restoration of indoor and outdoor monuments.

Canada, G. of, n.d. Basic requirements of preventive conservation - Preventive conservation guidelines for collections - Canada.ca [WWW Document]. URL https://www.canada.ca/en/conservation-institute/services/preventive-conservation/guidelines-collections/basic-requirements-preventive-conservation.html (accessed 10.24.20).

Çengel Afshin J, Y.A.G., n.d. Heat and Mass transfer. Fifth edition. New York : McGraw-Hill Higher Education, [2015] ©2015.

Ciulla, G., Lo Brano, V., Orioli, A., 2010. A criterion for the assessment of the reliability of ASHRAE conduction transfer function coefficients. Energy Build. 42, 1426–1436. https://doi.org/http://dx.doi.org/10.1016/j.enbuild.2010.03.012

Coleman, H.W., Steele, W.G., 2018. Appendix B: Taylor Series Method (Tsm) for Uncertainty Propagation. Exp. Validation, Uncertain. Anal. Eng. 311–323. https://doi.org/10.1002/9781119417989.app2

Crevello, G., Hudson, N., Noyce, P., 2015. Corrosion condition evaluations of historic concrete icons. Case Stud. Constr. Mater. 2, 2–10. https://doi.org/10.1016/j.cscm.2014.12.005

Díaz, J.A., Ramos, J.S., Delgado, M.C.G., García, D.H., Montoya, F.G., Domínguez, S.Á., 2018.

A daily baseline model based on transfer functions for the verification of energy saving. A case study of the administration room at the Palacio de la Madraza, Granada. Appl. Energy 224, 538–549. https://doi.org/10.1016/j.apenergy.2018.04.060

Douglas-Jones, R., Hughes, J.J., Jones, S., Yarrow, T., 2016. Science, value and material decay in the conservation of historic environments. J. Cult. Herit. 21, 823–833. https://doi.org/10.1016/j.culher.2016.03.007

Estado, J. del, 1985. Ley 16/1985, del Patrimonio Histórico Español, toriginal 20342–20352.

Evangelisti, L., Guattari, C., Asdrubali, F., 2019. On the sky temperature models and their influence on buildings energy performance: A critical review. Energy Build. 183, 607–625. https://doi.org/https://doi.org/10.1016/j.enbuild.2018.11.037

Fernández-Ahumada, L.M., Casares, F.J., Ramírez-Faz, J., López-Luque, R., 2017. Mathematical study of the movement of solar tracking systems based on rational models. Sol. Energy 150, 20–29. https://doi.org/https://doi.org/10.1016/j.solener.2017.04.006

Filippi, M., 2015. Remarks on the green retrofitting of historic buildings in Italy. Energy Build. 95, 15–22. https://doi.org/10.1016/j.enbuild.2014.11.001

Fregonese, L., Rosina, E., Adami, A., Bottacchi, M.C., Romoli, E., Lattanzi, D., 2018. Monitoring as strategy for planned conservation: the case of Sant'Andrea in Mantova (Mantua). Appl. Geomatics 10, 441–451. https://doi.org/10.1007/s12518-018-0240-4

Fung, I.W.H., Tsang, Y.T., Tam, V.W.Y., Xu, Y.T., Mok, E.C.K., 2017. A review on historic building conservation: A comparison between Hong Kong and Macau systems. Renew. Sustain. Energy Rev. 71, 927–942. https://doi.org/10.1016/j.rser.2016.12.121

Gallego-Cartagena, E., Morillas, H., Maguregui, M., Patiño-Camelo, K., Marcaida, I., Morgado-Gamero, W., Silva, L.F.O., Madariaga, J.M., 2020. A comprehensive study of biofilms growing on the built heritage of a Caribbean industrial city in correlation with construction materials. Int. Biodeterior. Biodegrad. 147, 104874. https://doi.org/10.1016/j.ibiod.2019.104874

Gentile, C., Saisi, A., 2013. Operational modal testing of historic structures at different levels of excitation. Constr. Build. Mater. 48, 1273–1285. https://doi.org/10.1016/j.conbuildmat.2013.01.013

Gómez-Plata, L., Tutikian, B.F., Pacheco, F., Oliveira, M.S., Murillo, M., Silva, L.F.O., Bergmann, C.P., 2019. Multianalytical approach of stay-in-place polyvinyl chloride formwork concrete exposed to high temperatures. J. Mater. Res. Technol. 9, 5045–5055. https://doi.org/10.1016/j.jmrt.2020.03.022

Gredilla, A., Fdez-Ortiz de Vallejuelo, S., Rodriguez-Iruretagoiena, A., Gomez, L., Oliveira, M.L.S., Arana, G., de Diego, A., Madariaga, J.M., Silva, L.F.O., 2019. Evidence of mercury sequestration by carbon nanotubes and nanominerals present in agricultural soils from a coal fired power plant exhaust. J. Hazard. Mater. 378, 120747. https://doi.org/10.1016/j.jhazmat.2019.120747

Hafez, A.Z., Soliman, A., El-Metwally, K.A., Ismail, I.M., 2017. Tilt and azimuth angles in solar energy applications – A review. Renew. Sustain. Energy Rev. 77, 147–168. https://doi.org/10.1016/J.RSER.2017.03.131

Hafez, A.Z., Yousef, A.M., Harag, N.M., 2018. Solar tracking systems: Technologies and trackers drive types – A review. Renew. Sustain. Energy Rev. 91, 754–782. https://doi.org/https://doi.org/10.1016/j.rser.2018.03.094

Hester, J., Prabhu, S., Atamturktur, S., Sorber, J., 2017. Remote and Wireless Long-term Vibration Monitoring of Historic Monuments. Procedia Eng. 199, 3302–3307. https://doi.org/10.1016/j.proeng.2017.09.416

Icomos, 2000. The Charter of Krakow 2000: principles for conservation and restoration of built heritage. Archaeol. Pol. 38, 5.

ICOMOS, 2005. Xi ' an Declaration on the Conservation of the Setting of Heritage Structures , Sites and Areas. Gen. Assem. ICOMOS 1–4.

Islam, N., Rabha, S., Silva, L.F.O., Saikia, B.K., 2019. Air quality and PM10-associated poly-aromatic hydrocarbons around the railway traffic area: statistical and air mass trajectory approaches. Environ. Geochem. Health 41, 2039–2053. https://doi.org/10.1007/s10653-019-00256-z

Jenkins, V., 2018. Protecting the natural and cultural heritage of local landscapes: Finding substance in law and legal decision making. Land use policy 73, 73–83. https://doi.org/10.1016/j.landusepol.2017.12.056

Jo, Y.H., Lee, C.H., 2014. Quantitative modeling of blistering zones by active thermography for deterioration evaluation of stone monuments. J. Cult. Herit. 15, 621–627. https://doi.org/10.1016/j.culher.2013.12.002

Kordatos, E.Z., Exarchos, D.A., Stavrakos, C., Moropoulou, A., Matikas, T.E., 2013. Infrared thermographic inspection of murals and characterization of degradation in historic monuments. Constr. Build. Mater. 48, 1261–1265. https://doi.org/10.1016/j.conbuildmat.2012.06.062

Lienhard, J.H., Lienhard, J.H., 2011. A heat transfer textbook. Dover Publications.

Lucchi, E., 2018. Review of preventive conservation in museum buildings. J. Cult. Herit. 29, 180–193. https://doi.org/10.1016/j.culher.2017.09.003

Maghrabi, A., Clay, R., 2011. Nocturnal infrared clear sky temperatures correlated with screen temperatures and GPS-derived PWV in southern Australia. Energy Convers. Manag. 52, 2925–2936. https://doi.org/https://doi.org/10.1016/j.enconman.2011.02.027

McAdams W, 1958. Heat Transmission, 3rd McGraw. ed.

Mesas-Carrascosa, F.J., Verdú Santano, D., de Larriva, J.E.M., Ortíz Cordero, R., Hidalgo Fernández, R.E., García-Ferrer, A., 2016. Monitoring heritage buildings with open source hardware sensors: A case study of the mosque-cathedral of Córdoba. Sensors (Switzerland) 16. https://doi.org/10.3390/s16101620

Moioli, R., Boniotti, C., Konsta, A., Pili, A., 2018. Complex properties management. J. Cult. Herit. Manag. Sustain. Dev. 8, 130–144. https://doi.org/10.1108/jchmsd-06-2017-0035

Morillas, H., Maguregui, M., Gallego-Cartagena, E., Huallparimachi, G., Marcaida, I., Salcedo, I., Silva, L.F.O., Astete, F., 2019. Evaluation of the role of biocolonizations in the conservation state of Machu Picchu (Peru): The Sacred Rock. Sci. Total Environ. 654, 1379–1388. https://doi.org/10.1016/j.scitotenv.2018.11.299

Morillas, H., Vazquez, P., Maguregui, M., Marcaida, I., Silva, L.F.O., 2018. Composition and porosity study of original and restoration materials included in a coastal historical construction. Constr. Build. Mater. 178, 384–392. https://doi.org/10.1016/j.conbuildmat.2018.05.168

Murillo A., M., Tutikian, B.F., Christ, R., Silva, L.F.O., Maschen, M., Gómez P., L., Oliveira, M.L.S., 2020. Analysis of the influence of thickness on fire reaction performance in polyisocyanurate core sandwich panels. J. Mater. Res. Technol. 9, 9487–9497. https://doi.org/10.1016/j.jmrt.2020.06.088

O'Grady, M., Lechowska, A.A., Harte, A.M., 2017. Quantification of heat losses through building envelope thermal bridges influenced by wind velocity using the outdoor infrared thermography technique. Appl. Energy 208, 1038–1052. https://doi.org/10.1016/J.APENERGY.2017.09.047

Oliveira, M.L.S., Dario, C., Tutikian, B.F., Ehrenbring, H.Z., Almeida, C.C.O., Silva, L.F.O., 2019a. Historic building materials from Alhambra: Nanoparticles and global climate change effects. J. Clean. Prod. 232, 751–758. https://doi.org/10.1016/j.jclepro.2019.06.019

Oliveira, M.L.S., Izquierdo, M., Querol, X., Lieberman, R.N., Saikia, B.K., Silva, L.F.O., 2019b. Nanoparticles from construction wastes: A problem to health and the environment. J. Clean. Prod. 219, 236–243. https://doi.org/10.1016/j.jclepro.2019.02.096

Oliveira, M.L.S., Tutikian, B.F., Milanes, C., Silva, L.F.O., 2020. Atmospheric contaminations and bad conservation effects in Roman mosaics and mortars of Italica. J. Clean. Prod. 248, 119250. https://doi.org/10.1016/j.jclepro.2019.119250

Pachta, V., Papayianni, I., 2017. The Study of the Historic Buildings of Eclecticism in Thessaloniki Under the Prism of Sustainability. Procedia Environ. Sci. 38, 283–289. https://doi.org/10.1016/j.proenv.2017.03.078

Plan, N., Preventive, F.O.R., 2011. National Plan for Preventive Conservation 1–42.

Prieto, A.J., Silva, A., de Brito, J., Macías-Bernal, J.M., Alejandre, F.J., 2017. Multiple linear regression and fuzzy logic models applied to the functional service life prediction of cultural heritage. J. Cult. Herit. 27, 20–35. https://doi.org/10.1016/j.culher.2017.03.004

Qian, X.-Y., Zhang, Q., Wilkinson, S., Achal, V., 2015. Cleaning of historic monuments: looking beyond the conventional approach? J. Clean. Prod. 101, 180–181. https://doi.org/10.1016/j.jclepro.2015.03.089

Ramírez, O., da Boit, K., Blanco, E., Silva, L.F.O., 2020. Hazardous thoracic and ultrafine particles from road dust in a Caribbean industrial city. Urban Clim. 33, 100655. https://doi.org/10.1016/j.uclim.2020.100655

Ramírez, O., Sánchez de la Campa, A.M., Amato, F., Moreno, T., Silva, L.F., de la Rosa, J.D., 2019. Physicochemical characterization and sources of the thoracic fraction of road dust in a Latin American megacity. Sci. Total Environ. 652, 434–446. https://doi.org/10.1016/j.scitotenv.2018.10.214

Report, A.P., 2001. European preventive conservation strategy project. H/TEK lnstitute of Art and Design, Lummetie 2, 01300 Vantaa Finland.

Rojas, J.C., Sánchez, N.E., Schneider, I., Oliveira, M.L.S., Teixeira, E.C., Silva, L.F.O., 2019. Exposure to nanometric pollutants in primary schools: Environmental implications. Urban Clim. 27, 412–419. https://doi.org/10.1016/j.uclim.2018.12.011

Romero, M., Pach, P., Margarita, C., Pinto, F., 2018. Operational Modal Analysis : A Tool for Assessing Changes on Structural Health State of Historical Constructions after Consolidation and Reinforcement Works — Jura Chapel (Jerez de la Frontera , Spain) 2018.

Saikia, B.K., Saikia, J., Rabha, S., Silva, L.F.O., Finkelman, R., 2018. Ambient nanoparticles/nanominerals and hazardous elements from coal combustion activity: Implications on energy challenges and health hazards. Geosci. Front. 9, 863–875. https://doi.org/10.1016/j.gsf.2017.11.013

Salazar-Hernández, C., Cervantes, J., Puy-Alquiza, M.J., Miranda, R., 2015. Conservation of building materials of historic monuments using a hybrid formulation. J. Cult. Herit. 16, 185–191. https://doi.org/10.1016/j.culher.2014.05.004

Santos, H., Valença, P., Fernandes, E.O., 2017. UNESCO's Historic Centre of Porto: Rehabilitation and Sustainability. Energy Procedia 133, 86–94. https://doi.org/10.1016/j.egypro.2017.09.375

Silva, L.F.O., Milanes, C., Pinto, D., Ramirez, O., Lima, B.D., 2020a. Multiple hazardous elements in nanoparticulate matter from a Caribbean industrialized atmosphere. Chemosphere 239, 124776. https://doi.org/10.1016/j.chemosphere.2019.124776

Silva, L.F.O., Pinto, D., Neckel, A., Dotto, G.L., Oliveira, M.L.S., 2020b. The impact of air pollution on the rate of degradation of the fortress of Florianópolis Island, Brazil. Chemosphere 251, 126838. https://doi.org/10.1016/j.chemosphere.2020.126838

Silva, L.F.O., Pinto, D., Neckel, A., Oliveira, M.L.S., 2020c. An analysis of vehicular exhaust derived nanoparticles and historical Belgium fortress building interfaces. Geosci. Front. 11, 2053–2060. https://doi.org/10.1016/j.gsf.2020.07.003

Silva, L.F.O., Pinto, D., Neckel, A., Oliveira, M.L.S., Sampaio, C.H., 2020d. Atmospheric nanocompounds on Lanzarote Island: Vehicular exhaust and igneous geologic formation interactions. Chemosphere 254, 126822. https://doi.org/10.1016/j.chemosphere.2020.126822

Skouri, S., Ben Haj Ali, A., Bouadila, S., Ben Salah, M., Ben Nasrallah, S., 2016. Design and construction of sun tracking systems for solar parabolic concentrator displacement. Renew. Sustain. Energy Rev. 60, 1419–1429. https://doi.org/10.1016/j.rser.2016.03.006

Stephenson, D.G., Mitalas, G.P., 1971. Calculation of heat conduction transfer functions for multilayers slabs. ASHRAE Trans. 77, 117–126.

Varas-muriel, M.J., Fort, R., 2018. Microclimatic monitoring in an historic church fitted with modern heating : Implications for the preventive conservation of its cultural heritage. Build. Environ. 145, 290–307. https://doi.org/10.1016/j.buildenv.2018.08.060

Wilcox, J., Wang, B., Rupp, E., Taggart, R., Hsu-Kim, H., Oliveira, M.L.S., Cutruneo, C.M.N.L., Taffarel, S., Silva, L.F.O., Hopps, S.D., Thomas, G.A., Hower, J.C., 2015. Observations and Assessment of Fly Ashes from High-Sulfur Bituminous Coals and Blends of High-Sulfur Bituminous and Subbituminous Coals: Environmental Processes Recorded at the Macro- and Nanometer Scale. Energy & Fuels 29, 7168–7177.

https://doi.org/10.1021/acs.energyfuels.5b02033
Yüceer, H., Ipekoğlu, B., 2012. An architectural assessment method for new exterior additions to historic buildings. J. Cult. Herit. 13, 419–425. https://doi.org/10.1016/j.culher.2011.12.002